Annales
Geophysicae

The structure of standing Alfvén waves in a dipole magnetosphere with moving plasma

D. A. Kozlov[1,3]**, A. S. Leonovich**[1,3]**, and J. B. Cao**[2,3]

[1]Institute of Solar-Terrestrial Physics (ISTP), Russian Academy of Sciences, Siberian Branch, Irkutsk, Russia
[2]Center for Space Science and Applied Research, Chinese Academy of Science, Beijing, China
[3]Russian-Chinese Joint Research Center on Space Weather

Abstract. The structure and spectrum of standing Alfvén waves were theoretically investigated in a dipole magnetosphere with moving plasma. Plasma motion was simulated with its azimuthal rotation. The model's scope allowed for describing a transition from the inner plasmasphere at rest to the outer magnetosphere with convecting plasma and, through the magnetopause, to the moving plasma of the solar wind. Solutions were found to equations describing longitudinal and transverse (those formed, respectively, along field lines and across magnetic shells) structures of standing Alfvén waves with high azimuthal wave numbers $m \gg 1$. Spectra were constructed for a number of first harmonics of poloidal and toroidal standing Alfvén waves inside the magnetosphere. For charged particles with velocities greatly exceeding the velocity of the background plasma, an effective parallel wave component of the electric field appears in the region occupied by such waves. This results in structured high-energy-particle flows and in the appearance of multiband aurorae. The transverse structure of the standing Alfvén waves' basic harmonic was shown to be analogous to the structure of a discrete auroral arc.

Keywords. Magnetospheric physics (Auroral phenomena; Magnetosphere-ionosphere interactions; MHD waves and instabilities)

1 Introduction

Alfvén oscillations in a magnetosphere are known to enjoy two types of polarisation (Dungey, 1954; Radoski, 1967, 1969). Oscillations in an axisymmetrical magnetosphere, exemplified by a dipole magnetic field model, may be represented as the sum of azimuthal harmonics of the form $\exp(im\phi)$, where m is the azimuthal wave number, ϕ is the azimuthal angle. Oscillations with $m \to \infty$ are termed toroidally polarised, while those with $m=0$ are poloidally

polarised oscillations. In toroidal Alfvén oscillations, the disturbed magnetic field and plasma fluctuate azimuthally, while the electric field fluctuates radially across magnetic shells. For poloidal oscillations the case is reversed: the magnetic field and plasma fluctuate radially, while the electric field fluctuates azimuthally. Each geomagnetic field line crosses the Earth's ionosphere in both the Northern and Southern Hemispheres. Alfvén oscillations, propagating chiefly along these field lines, form standing waves between the magnetoconjugated ionospheres.

Each magnetic shell was shown in Krylov et al. (1981) to be characterised by two sets of standing Alfvén wave eigenfrequencies. One corresponds to poloidal waves the other, to toroidal Alfvén waves. Alfvén oscillations with $m \neq 0, \infty$ are not purely poloidal or toroidal. Their polarisation may be chiefly poloidal/toroidal, depending on the ratio between their characteristic spatial scales in the azimuthal and radial directions.

The polarisation of standing Alfvén waves generated by the field line resonance mechanism, with $m \sim 1$, is almost toroidal (Southwood, 1974; Chen and Hasegawa, 1974; Leonovich and Mazur, 1989). A theory of such oscillations was originally developed for a one-dimensionally inhomogeneous model of the magnetosphere (Chen and Hasegawa, 1974; Southwood, 1974). Papers were published later in which this process was examined in models of a magnetosphere inhomogeneous along two coordinates – along magnetic field lines and across magnetic shells. A box model with straight magnetic field lines was discussed in Southwood and Kivelson (1986), a model of the magnetosphere as a semicylinder in Allan et al. (1986), and models with dipole magnetic field in Chen and Cowley (1989); Leonovich and Mazur (1989); Wright (1992).

Nonlinear effects in the resonant Alfvén waves proved to be very interesting and important for the dynamics of magnetospheric charged particles. Thus, ponderomotive forces arise in a nonlinear Alfvén wave (Rankin et al., 1994; Allan and Manuel, 1996), capable of accelerating electrons along magnetic field lines up to an energy of several kev.
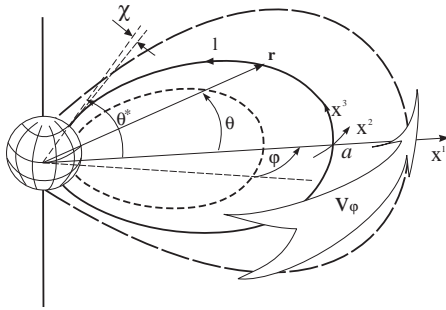
Correspondence to: A. S. Leonovich
(leon@iszf.irk.ru)

Fig. 1. A model magnetosphere with a dipole magnetic field and azimuthally rotating plasma ($\mathbf{v}=(0, v_\phi, 0)$). Coordinate systems tied to magnetic field lines are shown: a curvilinear orthogonal system of coordinates (x^1, x^2, x^3) and a non-orthogonal system of coordinates (a, ϕ, θ) used in numerical computations.

Precipitating in the ionosphere, these electrons are capable of triggering aurorae in polar latitudes. Taking into account dispersion kinetic effects in Alfvén waves allows a longitudinal electric field $E_\parallel$ to be revealed in these waves (Hasegawa, 1976; Goertz, 1984). In a nonlinear Alfvén wave, the $E_\parallel$ amplitude is one order of magnitude larger than in a linear one (Frycz et al., 1998). Taking into account the nonlocal conductivity effect for electrons in the field of a nonlinear Alfvén wave can increase $E_\parallel$ by several orders of magnitude (Rankin et al., 1999; Tikhonchuk and Rankin, 2000; Samson et al., 2003; Watt et al., 2004). This is related to the fact that, within one oscillation period of an Alfvén wave, electrons experience multiple bounce oscillations along field lines between the reflection points. Accelerated by the wave's longitudinal electric field, electrons can acquire energy necessary for aurorae to emerge in the ionosphere. Besides, kinetic dispersion effects and nonlinearities result in Alfvén oscillations being nonlinearly structured across magnetic shells (Rankin et al., 2004).

The structure of standing Alfvén waves with $m \gg 1$ is more complicated. They are excited by a monochromatic source as nearly poloidal oscillations on the magnetic shell whose source frequency coincides with a poloidal eigenfrequency of the Alfvén oscillations. Later on, they slowly (much slower than the Alfvén velocity) travel across magnetic shells to the shell whose toroidal eigenfrequency of Alfvén oscillations equals that of the source's frequency. Alfvén oscillations are entirely absorbed in the neighbourhood of this shell because of their dissipation in the ionosphere. In the process of this displacement, standing Alfvén waves change their polarisation from nearly poloidal to nearly toroidal (Leonovich and Mazur, 1993).

All the above-cited investigations involved model magnetospheres with quiescent plasma. The actual magnetosphere is a configuration with its plasma in dynamical equilibrium. In other words, motion is an inalienable property of the magnetospheric plasma. This factor is of doubtless importance in forming the structure and spectrum of the magnetosphere's Alfvén eigen oscillations. This work is a first-attempted

theoretical exploration of the effects taht the magnetospheric plasma motion exerts on the structure and spectrum of standing Alfvén waves with high azimuthal wave numbers $m \gg 1$. The research employed a self-consistent model magnetosphere with a dipole magnetic field, in which plasma motions were simulated by its azimuthal rotation (Leonovich et al., 2004).

The paper is structured as follows. Section 2 provides a brief description of the model magnetosphere, as well as deriving the principal equation describing the structure and spectrum of standing Alfvén waves with $m \gg 1$ in an axisymmetrical magnetosphere with rotating plasma. Section 3 explores the longitudinal structure (the one forming along field lines) and spectrum of standing Alfvén waves near a toroidal resonant shell. An equation is derived describing the structure of these oscillations across magnetic shells. Section 4 describes similar research carried out near a poloidal resonant shell. Section 5 produces a solution for the model equation describing the structure of monochromatic standing Alfvén waves across magnetic shells in the entire region of existence. Section 6 presents results of numerical calculations covering the spatial structure and spectrum of several first harmonics of these oscillations. Section 7 compares the standing Alfvén waves' spatial structure and propagation velocity to the structure and characteristic dynamics of discrete auroral arcs. The Conclusion lists the principal results of this research.

2 Model medium and major equations

To solve the problem posed, let us employ a model magnetosphere with a dipole magnetic field and azimuthally rotating plasma (Fig. 1). A self-consistent analytical model of such a magnetosphere was presented in Leonovich et al. (2004). Rotating plasma simulates both its convective motion inside the magnetosphere and the solar wind flow around the magnetosphere. Whereas plasma in the process is affected by centrifugal forces, the equilibrium of the plasma configuration is sustained by the gas-kinetic pressure gradient. This rather simple model allows for a realistic description of the distribution of plasma parameters in the dayside magnetosphere – the plasmapause and magnetopause included. Note that it is not the only possible way to construct a balanced axisymmetrical model with rotating plasma. Analogous models were presented in Bespalov and Chugunov (1984); Soldatkin and Chugunov (2003), where a system's dynamic equilibrium was sustained thanks to the Earth's gravity field and self-consistent generation of currents in a differentially rotating plasma. They are more sophisticated electrodynamic-equilibrium models. Our goals of exploring the plasma motion effect on the structure of standing Alfvén waves, however, are quite satisfied by using the above simpler model. It includes the actual magnetosphere's major elements necessary for the problem posed: a dipole magnetic field, a differentially rotating plasma and the presence of a gas-kinetic pressure gradient.

To examine Alfvén oscillations in this model, we will use the system of ideal MHD equations:

$$\rho \frac{d\mathbf{v}}{dt} = -\nabla P + \frac{1}{4\pi}[\text{curl } \mathbf{B} \times \mathbf{B}], \tag{1}$$

$$\frac{\partial \mathbf{B}}{\partial t} = \text{curl}[\mathbf{v} \times \mathbf{B}], \tag{2}$$

$$\frac{\partial \rho}{\partial t} + \nabla(\rho \mathbf{v}) = 0, \tag{3}$$

$$\frac{d}{dt} \frac{P}{\rho^\gamma} = 0, \tag{4}$$

where $\mathbf{B}$ and $\mathbf{v}$ are magnetic field vectors and plasma motion velocities, P and ρ are the plasma pressure and density, γ is the adiabatic index. In Eqs. (1) and (4), $d/dt = \partial/\partial t + (\mathbf{v}\nabla)$ represents the Lagrangian derivative in a moving plasma. In a steady state ($\partial/\partial t = 0$), the set of Eqs. (1–4) describes the distribution of the plasma equilibrium parameters $\mathbf{B}_0$, $\mathbf{v}_0$, P_0 and ρ_0.

We introduce a curvilinear orthogonal coordinate system (x^1, x^2, x^3) tied to magnetic field lines. The x^3 coordinate is directed along the field line, x^1 across magnetic shells, whereas x^2 is directed azimuthally and complements the coordinate system so that it becomes right-handed. In this system of coordinates $\mathbf{B}_0 = (0, 0, B_{03})$, $\mathbf{v}_0 = (0, v_{02}, 0)$, while the length element has the form

$$ds^2 = g_1(dx^1)^2 + g_2(dx^2)^2 + g_3(dx^3)^2,$$

where g_i ($i = 1, 2, 3$) are metrical tensor elements. Using the azimuthal angle ϕ as the azimuthal coordinate yields $v_{02} \equiv v_\phi = \sqrt{g_2}\Omega$, where Ω is the angular speed of the rotating plasma. Note that in the model under examination, the plasma rotation on each magnetic shell proceeds with a constant angular velocity $\Omega \equiv \Omega(x^1)$. The portion of the magnetosphere below the plasmapause, corresponding to the plasmasphere, is assumed to be at rest. Passing through the plasmapause, the plasma rotation velocity reaches $v_{02} \sim 30-50$ km/s, a value characteristic of convective plasma motion in the outer magnetosphere. Passing through the magnetopause, the plasma velocity increases to $v_{02} \approx 400$ km/s, typical of the solar wind.

We linearise the system of Eqs. (1–4) relative to the smaller disturbances due to the plasma MHD oscillations and consider the monochromatic oscillations of the form $\exp(-i\omega t + ik_2 x^2)$, where ω is the oscillation frequency, k_2 is the azimuthal wave vector (if $x^2 = \phi$ is the azimuthal angle, then $k_2 \equiv m = 0, \pm 1, \pm 2, \ldots$ is the azimuthal wave number). The first two equations Eq. (1) yield

$$-\rho_0(i\bar{\omega}v_1 + v_2\Omega\nabla_1 \ln g_2) - \frac{\tilde{\rho}\Omega^2}{2}\nabla_1 g_2 =$$
$$-\nabla_1 \tilde{P} - \frac{B_0}{4\pi}\frac{1}{\sqrt{g_3}}(\nabla_3 B_1 - \nabla_1 B_3), \tag{5}$$

$$\rho_0\left(-i\bar{\omega}v_2 + v_1\frac{\nabla_1(g_2\Omega)}{g_1} + \frac{v_3\Omega}{g_3}\nabla_3 g_2\right) =$$
$$-ik_2\tilde{P} - \frac{B_0}{4\pi}\frac{1}{\sqrt{g_3}}(ik_2 B_3 - \nabla_3 B_2), \tag{6}$$

where $\nabla_i \equiv \partial/\partial x^i$ ($i = 1, 2, 3$), while v_i and B_i are the disturbed velocity and disturbed magnetic field vector components, $\tilde{P}$ and $\tilde{\rho}$ are the plasma's disturbed pressure and density. The added notation $\bar{\omega} = \omega - m\Omega$ here refers to the Doppler-shifted oscillation frequency in rotating plasma.

To describe MHD perturbations propagating in the plasma, it is convenient to switch from the components of the electromagnetic field and disturbed velocity field to potentials. According to the Helmholtz expansion theorem (Korn and Korn, 1968), an arbitrary vector field can be represented as the sum of the vortex-free and solenoidal fields.

We represent the disturbed electric field of the oscillations as

$$\mathbf{E} = -\nabla\varphi + \text{curl } \Psi,$$

where φ is the scalar potential, and $\Psi = (\psi_1, \psi_2, \psi_3)$ is the vector potential. This obviously implies that $\mathbf{E}$ is invariant to an arbitrary constant added to the scalar potential $\varphi \to \varphi + \text{const}$ and to an arbitrary gradient added to the vector potential $\Psi \to \Psi + \nabla\chi$. Without loss of generality, one can choose const $= 0$, while choosing $\nabla\chi$ such that $\psi_1 + \nabla_1\chi = 0$, i.e. $\Psi = (0, \xi, \psi)$, where $\xi = \psi_2 + \nabla_2\chi$, $\psi = \psi_3 + \nabla_3\chi$.

The electric, $\mathbf{E}$, the magnetic, $\mathbf{B}$, and velocity $\mathbf{v}$, fields of oscilations are related by Eqs. (2), and by the equation

$$\mathbf{E} = -\frac{1}{c}(\mathbf{v} \times \mathbf{B}_0 + \mathbf{v}_0 \times \mathbf{B}),$$

that allow for the components of $\mathbf{B}$ and $\mathbf{v}$ to be expressed in terms of the potentials φ, ξ and ψ. Based on Eqs. (3) and (4), one can also express the disturbed density $\tilde{\rho}$ and the pressure $\tilde{P}$ in terms of the potentials.

We will focus our interest on oscillations with $m \gg 1$ in the neighbourhood of resonant surfaces. As further calculations will show, the potential φ has a singularity on these surfaces. The field of resonant Alfvén oscillations can be expressed through it.

The potentials ξ and ψ have no such singularities and, in zero approximation, can be neglected. Note that it can only be done for oscillations with $m \gg 1$. When $m \sim 1$, the potential ψ, that describes magnetosonic oscillations as well, can play the role of a source for Alfvén waves via the field-line resonance mechanism. While $m \gg 1$, magnetosonic oscillations practically do not penetrate the magnetosphere and are unable to effectively excite Alfvén waves (Leonovich and Mazur, 2000).

The expressions for components of the Alfvén oscillations' electromagnetic and velocity fields associated with the potential φ are:

$$E_1 = -\nabla_1\varphi, \quad E_2 = -ik_2\varphi, \quad E_3 = \frac{k_2\Omega}{\bar{\omega}}\nabla_3\varphi,$$

$$B_1 = \frac{k_2 c}{\bar{\omega}}\frac{g_1}{\sqrt{g}}\nabla_3\varphi,$$

$$B_2 = i\frac{c}{\bar{\omega}}\frac{g_2}{\sqrt{g}}\nabla_3\left(\nabla_1 - k_2\frac{\Omega'}{\bar{\omega}}\right)\varphi, \quad B_3 = 0,$$

$$v_1 = -i\frac{k_2}{p}\frac{c}{B_0}\varphi, \quad v_2 = \frac{cp}{B_0}\nabla_1\varphi,$$

$$v_3 \approx i \frac{cp}{B_0} \frac{\Omega}{\bar{\omega}} (\nabla_3 \ln g_2) \nabla_1 \varphi, \tag{7}$$

where $g = g_1 g_2 g_3$, $\Omega' \equiv \nabla_1 \Omega$. Note that a stationary system of coordinates associated with Earth witnesses the emergence of longitudinal components of the electric field of oscillations $E_3 \neq 0$ and of the velocity field $v_3 \neq 0$. This effect can prove to be of importance in the dynamics of the magnetospheric plasma ions and electrons, and in their precipitation into the ionosphere. Until now, the presence of $E_\parallel$ and $v_\parallel$ in Alfvén waves has been thought to be associated with small kinetic effects, such as a finite ion Larmor radius or electron skin-length (Hasegawa, 1976; Goertz, 1984). It follows from Eq. (7), for particles that are at rest relative to Earth (but moving relative to the background magnetospheric plasma), $E_\parallel / E_\perp \sim v_\parallel / v_\perp \sim v_\phi / A$ in order of magnitude.

To obtain an equation for Alfvén waves, let us multiply Eq. (5) by $ik_2 B_0 / \rho_0$, and Eq. (6) by B_0 / ρ_0, take a derivative ∇_1 of Eq. (6) and subtract Eq. (6) from Eq. (5). For virtually the entire magnetosphere the inequality $S, v_{20} \ll A$ holds true, where A is the Alfvén velocity, $S = \sqrt{\gamma P_0 / \rho_0}$ is the sound velocity in plasma. Therefore, terms of order S/A and v_{02}/A will be assumed to be small. The resulting equation for transverse small-scale ($m \gg 1$) Alfvén waves has the form:

$$\nabla_1 \widehat{L}_T \nabla_1 \varphi - k_2^2 \widehat{L}_P \varphi + k_2 \frac{\nabla_1 \Omega}{\bar{\omega}} \nabla_1 \widehat{L}_{T0} \varphi = 0, \tag{8}$$

where

$$\widehat{L}_T = \widehat{L}_{T0} - \beta_T,$$
$$\widehat{L}_P = \widehat{L}_{P0} - \beta_P,$$

are the toroidal and poloidal longitudinal operators

$$\widehat{L}_{T0} = \frac{1}{\sqrt{g_3}} \nabla_3 \frac{p}{\sqrt{g_3}} \nabla_3 + p \frac{\bar{\omega}^2}{A^2},$$
$$\widehat{L}_{P0} = \frac{1}{\sqrt{g_3}} \nabla_3 \frac{p^{-1}}{\sqrt{g_3}} \nabla_3 + p^{-1} \frac{\bar{\omega}^2}{A^2},$$

are the zero approximation operators in a cold ($P_0 = 0$) stationary ($\Omega = 0$) plasma,

$$\beta_T = p \frac{\Omega^2}{A^2} \left(\frac{\nabla_3 g_2}{\sqrt{g_2 g_3}} \right)^2,$$

$$\beta_P = p \frac{\Omega^2}{2A^2} (\nabla_1 \ln g_2) \left(\nabla_1 \ln \frac{\rho_0 \sqrt{g_3}}{B_0} \right) +$$
$$+ \frac{S^2}{A^2} \frac{\nabla_1 \ln \bar{\omega} / B_0}{\sqrt{g_1 g_2}} \left(\nabla_1 \ln \frac{P_0^{1/\gamma} \sqrt{g_3}}{B_0} \right),$$

are the corrections due to the plasma motion and pressure.

The additional notation $p = \sqrt{g_2 / g_1}$ is used here. As long as we are examining transverse small-scale oscillations, Eq. (8) retains only the basic terms quadratic on transverse derivatives ($\nabla_1 \varphi$, $\nabla_2 \varphi$). If the plasma is cold ($P_0 = 0$) and stationary ($\Omega = 0$), Eq. (8) transforms into the familiar equation describing the structure of Alfvén oscillations with $m \gg 1$ in a cold plasma (Leonovich and Mazur, 1993). Analogous

research in the stationary magnetosphere with plasma under pressure other than zero was conducted in Klimushkin (1997). For $\Omega = 0$, $P_0 \neq 0$, Eq. (8) transforms into a corresponding equation of that paper.

3 The structure of Alfvén oscillations near a poloidal resonant surface

As was shown in Leonovich and Mazur (1993), transverse, small-scale Alfvén waves can be excited in the neighbourhood of a poloidal resonant surface only. Their source cannot be provided by fast magnetosonic waves generated outside the magnetosphere or at its boundary with the solar wind. Magnetosonic oscillations with $m \gg 1$ practically do not penetrate the magnetosphere. A possible source of such oscillations can be the ring current, appearing during geomagnetic disturbances (Pilipenko, 1990). External currents in the ionosphere were discussed in Leonovich and Mazur (1993) as a source of standing Alfvén waves with $m \gg 1$. This paper also assumes such external currents to be present.

In this case, the boundary condition for the potential φ has the form (Leonovich and Mazur, 1996):

$$\varphi|_{x_\pm^3} = \mp \frac{v_\pm}{\bar{\omega}} \frac{1}{\sqrt{g_3}} \frac{\partial \varphi}{\partial x^3} \bigg|_{x_\pm^3} - \frac{J_\parallel^\pm}{V_\pm} \tag{9}$$

on the ionosphere, where the notations are:

$$v_\pm = \frac{c^2 \cos \chi_\pm}{4\pi \Sigma_p^\pm}, \quad V_\pm = \frac{\Sigma_p^\pm}{\cos \chi_\pm} .$$

The signs $\pm$ refer to the Northern and Southern Hemispheres, χ is the angle between the vertical and the field line at its intersection point with the ionosphere, Σ_p is the integrated Pedersen conductivity in the ionosphere, while the function $J_\parallel$ is related to the density $j_\parallel$ of external field-aligned currents in the topside ionosphere by

$$\Delta_\perp J_\parallel = j_\parallel,$$

where $\Delta_\perp = \nabla_1^2 / g_1 - k_2^2 / g_2$ is the transverse Laplacian. The right-hand terms in Eq. (9) will be assumed to be small, implying the values of the parameters $v_\pm$ and $1/V_\pm$ to be small, too.

The calculations that follow below will involve the basic and several first harmonics of standing Alfvén waves. Since we assume Alfvén oscillations across magnetic shells to be small-scale, the characteristic wave length on x^1 coordinate is much smaller than the longitudinal wave length on x^3 coordinate. In this context, the solution to Eq. (8) can be sought in the form:

$$\varphi = U(x^1) H(x^1, x^3) \exp(ik_2 x^2 - i\omega t), \tag{10}$$

where the function $U(x^1)$ describes the small-scale structure of oscillations across magnetic shells, while $H(x^1, x^3)$ describes their structure along geomagnetic field lines. The scale of variations of H on x^1, in the meantime,
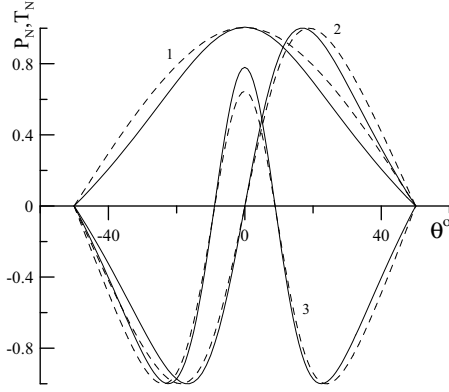
Fig. 2. The structure of standing Alfvén waves with toroidal (solid lines) and poloidal polarisation (dashed lines). The curves are of the poloidal, P_N, and toroidal, T_N, eigenfunctions with unity amplitude for the first three parallel harmonics ($N = 1, 2, 3$).
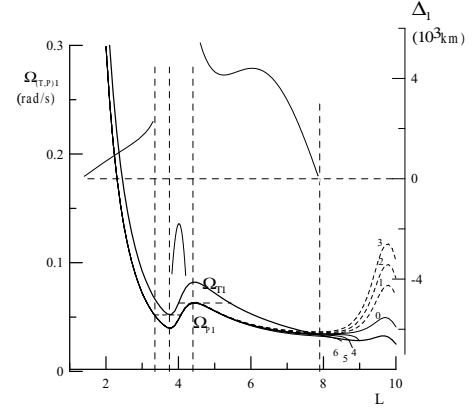

Fig. 3. Dependency of the toroidal and poloidal eigenfrequencies $\Omega_{TN}(x^1)$, $\Omega_{PN}(x^1)$ (the lower curves) on the magnetic shell parameter L for the first parallel harmonic of Alfvén oscillations, $N=1$. The numbers 0, 1, 2, ..., 6 refer to curves of poloidal eigenfrequencies with various values of azimuthal wave number: (0) $m=0$, (1) $m=-20$, (2) $m=-50$, (3) $m=-100$, (4) $m=20$, (5) $m=50$, (6) $m=100$. The upper curve displays the dependency of equatorial distance between the poloidal and toroidal resonant shells.
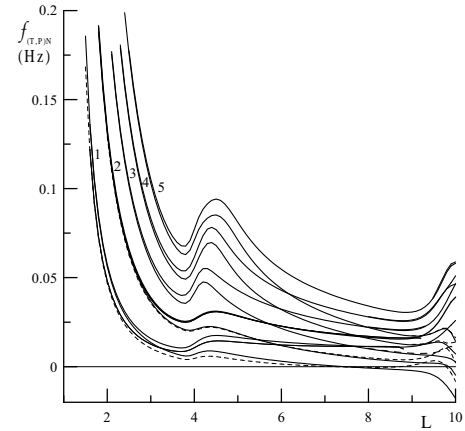
significantly exceeds the scale of variations of $U(x^1)$: $|\nabla_1 U/U| \gg |\nabla_1 H/H|$. Justification of the desired solution in the form Eq. (10) is given in more detail in Leonovich and Mazur (1993).

In the neighbourhood of a poloidal resonant surface, the azimuthal wave length is much smaller than the radial: $k_2^2 \gg |\nabla_1 U/U|^2$. The second term in Eq. (8), therefore, begins to greatly exceed the other two. The function $H(x^1, x^3)$ in the neighbourhood of a poloidal resonant surface is represented as

$$H(x^1, x^3) = P(x^1, x^3) + h(x^1, x^3),$$

where $P(x^1, x^3)$ is a function describing the longitudinal structure of standing Alfvén waves and satisfying, in the main order of perturbation theory, the equation:

$$\widehat{L}_P P = 0. \tag{11}$$

Boundary conditions on the ionosphere for function $P(x^1, x^3)$, in the same approximation, have the form

$$P(x^1, x_\pm^3) = 0. \tag{12}$$

The solution of Eqs. (11), (12) are the poloidal eigenfunctions $P_N(x^1, x^3)$ and the corresponding eigenvalues $\bar{\omega} \equiv \Omega_{PN}(x^1)$, where $N=1, 2, \ldots$ is the longitudinal wave number (the number of nodes of the function $P_N(x^1, x^3)$ on the field line being $N - 1$). Let us define the normalisation of the function $P_N(x^1, x^3)$ with the following condition

$$\int_{\ell_-}^{\ell_+} P_N^2 \frac{p^{-1}}{A^2} d\ell = 1, \tag{13}$$

where integration is along a field line, whose length element $d\ell = \sqrt{g_3} dx^3$, while $\ell_\pm$ correspond to its intersection points with the ionosphere in the Northern and Southern Hemispheres.

Fig. 4. Dependency of the toroidal (thick lines) and poloidal (thin lines) eigenfrequencies $\Omega_{TN}(x^1)$, $\Omega_{PN}(x^1)$ on the magnetic shell parameter L for the first five longitudinal harmonics ($N=1, \ldots, 5$), in the source reference frame. The poloidal eigenfrequency values shown correspond to the azimuthal harmonics $m=50$ (solid lines) and $m=, -50$ (dashed lines).

The numerical solution of Eqs. (11), (12) is shown in Figs. 2, 3 and 4. Figure 2 shows the structure of oscillations along field lines (function $P_N(x^1, x^3)$), whereas Figs. 3 and 4 depict the dependence of the eigenvalues Ω_{PN} on the magnetic shell parameter L (Figure 3 displays the basic harmonic $\Omega_{P1}(L)$, while Fig. 4 shows $f_{PN} = (\Omega_{PN} - m\Omega)/2\pi$, $N=1, 2, 3, 4, 5$). The solutions obtained are discussed in more detail in Sect. 6.

Function $h(x^1, x^3)$ corrects $P(x^1, x^3)$ in the higher orders of perturbation theory. Boundary conditions for it have the

form

$$h_N(x^1, \ell_\pm) = \mp \frac{v_\pm}{\Omega_{PN}} \frac{\partial P_N}{\partial \ell} \bigg|_{\ell_\pm} - \frac{J_\parallel^\pm}{U_N(x^1)V_\pm}. \quad (14)$$

In the first order of perturbation theory, Eq. (8) serves to obtain the equation

$$\nabla_1 \widehat{L}_T(\Omega_{PN}) P_N \nabla_1 U_N - k_2^2 U_N \widehat{L}_P(\Omega_{PN}) h_N -$$

$$k_2^2 U_N \frac{p^{-1}}{A^2} (\bar{\omega}^2 - \Omega_{PN}^2) P_N +$$

$$\frac{k_2 \Omega'}{\Omega_{PN}} \widehat{L}_T(\Omega_{PN}) P_N \nabla_1 U_N = 0.$$

Premultiplying this equation by P_N and integrating it along a field line between the magnetoconjugated ionospheres yields, in view of the normalisation condition Eq. (13):

$$\alpha_{PN} \nabla_1^2 U_N - k_2^2 [(\bar{\omega} + i\gamma_{PN})^2 - \Omega_{PN}^2] U_N +$$

$$\alpha_{PN} \frac{k_2 \Omega'}{\Omega_{PN}} \nabla_1 U_N = I_N, \quad (15)$$

where the notations are:

$$\alpha_{PN} = \int_{\ell_-}^{\ell_+} P_N^2 \left(\frac{\partial^2 p}{\partial \ell^2} + \beta_P \right) d\ell,$$

$$\gamma_{PN} = \frac{1}{2\Omega_{PN}^2} \left[\frac{v_+}{p_+} \left(\frac{\partial P_N}{\partial \ell} \right)_{\ell_+} + \frac{v_-}{p_-} \left(\frac{\partial P_N}{\partial \ell} \right)_{\ell_-} \right],$$

$$I_N = \left[\frac{j_\parallel^{(+)}}{V_+} \sqrt{g_1 g_2} \left(\frac{\partial P_N}{\partial \ell} \right)_{\ell_+} - \frac{j_\parallel^{(-)}}{V_-} \sqrt{g_1 g_2} \left(\frac{\partial P_N}{\partial \ell} \right)_{\ell_-} \right].$$

One can see from Eq. (15) that γ_{PN} acts as a decrement of poloidal Alfvén waves, determined by their Joule dissipation in the ionosphere. Function I_N represents a source of oscillations linked to external currents in the ionosphere. Equation (15) describes the structure of standing Alfvén waves across magnetic shells near a poloidal resonant surface. A solution to Eq. (15) may be found by linearising the coefficients in the neighbourhood of the poloidal resonant surface $x^1 = x_{PN}^1$ (where $\bar{\omega} = \Omega_{PN}(x_{PN}^1)$). An analogous solution can be construed near a toroidal resonant surface $x^1 = x_{TN}^1$ (where $\bar{\omega} = \Omega_{TN}(x_{TN}^1)$) as well, and these solutions are later matched together across the gap using the WKB approximation on x^1 coordinate. This rather unwieldy technique was implemented in Leonovich and Mazur (1993). This paper applies a different approach. Section 5 proposes a model equation describing the structure of standing Alfvén waves across magnetic shells in the entire region of existence, including the poloidal and toroidal resonant surfaces. An analytical solution is found for this equation in the same section.

4   The structure of Alfvén oscillations near toroidal resonant surfaces

Near toroidal resonant surfaces, the characteristic wave length (on x^1 coordinate) of the Alfvén oscillations across magnetic shells under study is much smaller than that on the azimuthal x^2 coordinate. The Alfvén oscillations are generated considerably less effectively near the toroidal surface than near the poloidal (Leonovich and Mazur, 1993). Therefore, in the neighbourhood of the toroidal surface in the boundary condition (9), the last term, related to external currents in the ionosphere, can be ignored. Represent function $H(x^1, x^3)$, describing the structure of oscillations along a field line near the toroidal surface, as:

$$H(x^1, x^3) = T(x^1, x^3) + h(x^1, x^3).$$

Here, the function $T(x^1, x^3)$ satisfies the zero-order equation

$$\widehat{L}_T T = 0, \quad (16)$$

with homogeneous boundary conditions on the ionosphere

$$T(x^1, x_\pm^3) = 0. \quad (17)$$

The solution of Eqs. (16), (17) is represented by toroidal eigenfunctions $T_N(x^1, x^3)$ ($N=1, 2, \ldots$ being the longitudinal wave number), with corresponding eigenvalues $\bar{\omega} = \Omega_{TN}(x^1)$. A numerical solution for Eqs. (16), (17) is shown in Fig. 2 (eigenfunctions) and Figs. 3, 4 (eigenvalues). These figures exhibit the structures of poloidal and toroidal Alfvén waves along magnetic field lines as fairly similar. Nor is there much difference between the eigenfrequencies of the poloidal and toroidal oscillations. The exception is the basic harmonic $N=1$, for which the eigenfrequency splitting $\Delta \Omega_1 = \Omega_{T1} - \Omega_{P1}$ can reach a quarter of their value. Choose the normalisation of eigenfunctions $T_N(x^1, x^3)$ in the form

$$\int_{\ell_-}^{\ell_+} T_N^2 \frac{p}{A^2} d\ell = 1. \quad (18)$$

We obtain from Eq. (8), in the first order of perturbation theory, an equation for the function $U_N(x^1)$:

$$T_N \nabla_1 \frac{p}{A^2} (\bar{\omega}^2 - \Omega_{TN}^2) \nabla_1 U_N - k_2^2 U_N \widehat{L}_P(\Omega_{TN}) T_N +$$

$$\nabla_1^2 U_N \widehat{L}_T(\Omega_{TN}) h_N = 0, \quad (19)$$

describing the structure of oscillations across magnetic shells near the toroidal resonant surface. Equation (19) is premultiplied by T_N and integrated along a field line between the magnetoconjugated ionospheres. Given the boundary condition on the ionosphere Eq. (9), without the last term and the normalisation condition Eq. (18), we obtain

$$\nabla_1 [(\bar{\omega} + i\gamma_{TN})^2 - \Omega_{TN}^2] \nabla_1 U_N - k_2^2 \alpha_{TN} U_N = 0, \quad (20)$$

where

$$\alpha_{TN} = -\int_{\ell_-}^{\ell_+} T_N^2 \frac{\partial^2 p^{-1}}{\partial \ell^2} d\ell,$$

$$\gamma_{TN} = \frac{1}{2\Omega_{TN}^2}\left[v_+ p_+ \left(\frac{\partial T_N}{\partial \ell}\right)_{\ell_+} + v_- p_- \left(\frac{\partial T_N}{\partial \ell}\right)_{\ell_-}\right].$$

The function γ_{TN} constitutes a decrement for toroidal Alfvén waves due to their dissipation in the ionosphere. The next section will rely on Eqs. (15) and (20) to propose a model equation describing the structure of standing Alfvén waves across magnetic shells in the entire region of existence.

5 The structure of standing Alfvén waves across magnetic shells

A technique was developed in Leonovich and Mazur (1997) for describing the structure of standing Alfvén waves across magnetic shells by means of a model equation. Combining Eqs. (15) and (20), describing the structure of oscillations in the neighbourhood of the poloidal and toroidal resonant shells, one can construct a model equation

$$\sqrt{\alpha_{PN}}\nabla_1[(\bar{\omega}+i\gamma_N)^2 - \Omega_{TN}^2]\nabla_1 U_N -$$
$$\sqrt{\alpha_{PN}}\frac{k_2\Omega'}{\bar{\omega}}[(\bar{\omega}+i\gamma_N)^2 - \Omega_{TN}^2]\nabla_1 U_N -$$
$$\sqrt{\alpha_{TN}}k_2^2[(\bar{\omega}+i\gamma_N)^2 - \Omega_{PN}^2]U_N = \sqrt{\alpha_{TN}}I_N, \quad (21)$$

applicable for the entire region of existence. The same notations are used here as in the two previous sections. The only exception is the decrement γ_N, which we will deem the same for both the poloidal and toroidal oscillations.

Figures 3, 4 imply that a situation is typical for most of the magnetosphere when $\Omega_{PN}(x^1) > \Omega_{TN}(x^1)$. Consider just such regions of the magnetosphere. Since the functions $\Omega_{PN}(x^1)$ and $\Omega_{TN}(x^1)$ are similar enough, the characteristic scale of their variation on x^1 coordinate is virtually the same. Let the source (external currents in the ionosphere) generate a monochromatic oscillation in the magnetosphere, with a certain value of the azimuthal wave number m. In this case, standing Alfvén waves are excited near the resonant surface, where $\bar{\omega}=\omega-m\Omega=\Omega_{PN}(x^1)$. Expanding the function $\Omega_{PN}(x^1)$ near this surface down to linear terms yields

$$\Omega_{PN}(x^1) \approx \bar{\omega}\left(1 - \frac{x^1 - x_{PN}^1}{L}\right), \quad (22)$$

where L is the characteristic variation scale of $\Omega_{PN}(x^1)$ near $x^1 = x_{PN}^1$. This representation is obviously not to be applied near the extrema of the function $\Omega_{PN}(x^1)$, where $L \to \infty$. Analogously, one can factorise the function $\Omega_{TN}(x^1)$ in the neighbourhood of the toroidal resonant surface (where $\bar{\omega}=\Omega_{TN}(x^1)$):

$$\Omega_{TN}(x^1) \approx \bar{\omega}\left(1 - \frac{x^1 - x_{TN}^1}{L}\right). \quad (23)$$

Denote the equatorial distance between the toroidal and poloidal resonant surfaces as $\Delta_N = x_{TN}^1 - x_{PN}^1$. In Figs. 3 and 5, Δ_N corresponds to the distance between the intersection points of the horizontal line $\bar{\omega}=$const with the

$\Omega_{PN}(x^1)$ and $\Omega_{TN}(x^1)$ curves. Equations (22) and (23) imply that, in linear approximation, $\Delta_N \approx \Delta\Omega_N L/\bar{\omega}$, where $\Delta\Omega_N = \Omega_{TN} - \Omega_{PN}$ is the polarisation splitting of the spectrum.

Since we are to apply Eq. (21) near the poloidal and toroidal resonant surfaces, just a small distance apart ($\Delta_N \ll L$), we substitute the expansions Eqs. (22) and (23) into it. Switching to the dimensionless transverse coordinate $\xi = (x^1 - x_{TN}^1)/\Delta_N$, we obtain

$$\frac{\partial}{\partial\xi}(\xi+i\varepsilon)\frac{\partial U_N}{\partial\xi} + q(\xi+i\varepsilon)\frac{\partial U_N}{\partial\xi} - \kappa_N^2(\xi+1+i\varepsilon)U_N = b_N, \quad (24)$$

where the following dimensionless parameters are introduced

$$\varepsilon = 2\frac{\gamma_N}{\bar{\omega}}\frac{L}{\Delta_N}, \quad q = k_2\Delta_N\Omega'/\bar{\omega}, \quad \kappa_N^2 = \sqrt{\frac{\alpha_{TN}}{\alpha_{PN}}}k_2^2\Delta_N^2,$$

$$b_N = I_N\sqrt{\frac{\alpha_{TN}}{\alpha_{PN}}}\frac{L\Delta_N}{\bar{\omega}^2}.$$

A solution to Eq. (24) may be found using a Fourier transform:

$$U_N(\xi) = \frac{1}{\sqrt{2\pi}}\int_{-\infty}^{\infty}\bar{U}_N(k)e^{ik\xi}dk. \quad (25)$$

Substituting Eq. (25) into Eq. (24) can produce a first-order equation for the Fourier harmonic $\bar{U}_N$, to be easily solved (Leonovich and Mazur, 1997). Substituting the expression found for $\bar{U}_N(k)$ into Eq. (25) yields a solution to the initial Eq. (24) in the form:

$$U_N(\xi) = i\frac{b_N}{\kappa_N}\int_0^{\infty}\frac{\exp[ik(\xi+i\varepsilon)+i\alpha_N\arctan\psi(k)]}{\sqrt{k^2-ikq+\kappa_N^2}}dk, \quad (26)$$

where

$$\alpha_N = \frac{\kappa_N^2+q/2}{\sqrt{\kappa_N^2+q^2/4}}, \quad \psi(k) = k\frac{\sqrt{\kappa_N^2+q^2/4}}{\kappa_N^2-ikq/2}.$$

Let us consider the behaviour of the solution (26) near the toroidal resonant surface ($\xi \to 0$), as well as on asymptotics $|\xi| \to \infty$. With $\xi \to 0$, the bulk of the integral in Eq. (26) accumulates thanks to high values of $k \gg \kappa_N$. Letting $k \to \infty$ in the denominator (26) and in $\psi(k)$ produces an expression for both the derivative

$$\frac{\partial U_N}{\partial\xi}\underset{\xi\to 0}{\approx}\frac{b_N}{\kappa_N(\xi+i\varepsilon)}e^{i\alpha_N\arctan\psi(\infty)},$$

and the function itself

$$U_N\underset{\xi\to 0}{\approx}\frac{b_N}{\kappa_N}e^{i\alpha_N\arctan\psi(\infty)}\ln(\xi+i\varepsilon).$$

One can see that for $\varepsilon=0$, $U_N(\xi)$ on the toroidal resonant surface ($\xi \to 0$) has a logarithmic singularity known for resonant Alfvén waves.

Conversely, with $|\xi| \to \infty$, it is the values of $k \ll \kappa_N$ that make the greatest contribution into the integral Eq. (26). Therefore, we could set $k=0$ in the denominator of the integrand in Eq. (26) and in $\psi(k)$, resulting in

$$U_N(\xi) \underset{|\xi| \to \infty}{\approx} -\frac{b_N}{\kappa_N^2} \frac{1}{\xi + i\varepsilon}$$

– the asymptotics for high values of ξ. Thus, while $\varepsilon=0$, the function $U_N(\xi)$ has a singularity on the toroidal resonant surface, and linearly decreases in amplitude when moving away from it.

Figure 6 shows a typical behaviour of the function $U_N(\xi)$, describing the structure of the N-th harmonic of standing Alfvén waves across magnetic shells, for the two extreme values of the parameter: $\kappa_N \gg 1$ and $\kappa_N \ll 1$. Figure 6a provides a solution corresponding to $\kappa_N=0.1$, while Fig. 6b to $\kappa_N=20$. The decrement was chosen to be very small ($\varepsilon=10^{-3}$), in order to reveal the role of the parameter κ_N, acting as the wave number on ξ coordinate.

For $\kappa_N \gg 1$ the solution is a wave travelling from the poloidal ($\xi=-1$) to the toroidal resonant surface ($\xi=0$). This is evident from the phases $\text{Re}\,U_N$ and $\text{Im}\,U_N$ differing by $\sim \pi/2$ in the interval $-1 < \xi < 0$. This can easily be shown analytically by computing the integral (26) for $\kappa_n \to \infty$ using the saddle point method. With $\kappa_n \ll 1$ the oscillations' harmonic structure vanishes, and they become typical resonant oscillations, analogous to those in field line resonance. In the neighbourhood of a resonance peak the polarisation of oscillations is toroidal.

The critical value of κ_{Nc}, discriminating between the two above discussed structure types of standing Alfvén waves, equals 1. The value of κ_{Nc} is determined on each magnetic shell by the value of the critical azimuthal wave number m_c. Figure 7 illustrates the dependence of m_c on the magnetic shell parameter L for the first five harmonics of standing Alfvén waves. When $m \gg m_c$, the standing Alfvén wave has the form of a wave travelling across magnetic shells, while for $m \ll m_c$, the form of resonant oscillations. In reality, however, the structure of oscillations across magnetic shells is affected by their dissipation in the ionosphere, as well. When a certain value is exceeded, it is dissipation that determines the characteristic scale and structure of oscillations across magnetic shells.

6 Results of numerical computations and their discussion

Let us discuss in more detail the results in previous sections from numerical solutions of equations describing the longitudinal and transverse structure of standing Alfvén waves. Figure 2 presents the structure of the first three harmonics of standing Alfvén waves along magnetic field lines on the magnetic shell $L=3$ ($L=a/R_E$, where a is the equatorial radius of the magnetic shell, R_E is the Earth's radius). Here one should take notice of the fact that the structure of the same longitudinal harmonics is virtually identical between the poloidal and toroidal oscillations. This makes it possible, when describing the transverse structure of oscillations, to use a model equation applicable over the entire region of existence.

Figure 3 displays the curves for $\Omega_{P1}(x^1)$ and $\Omega_{T1}(x^1)$, as well as the equatorial splitting of resonant shells $\Delta_1(x^1)$ for the standing Alfvén waves' basic harmonic $N=1$. Discussing this harmonic separately is justified by its possessing a uniquely high value of the polarisation splitting of eigenfrequencies $\Delta\Omega_1=\Omega_{T1}-\Omega_{P1}$ and of the associated resonant shell splitting Δ_1. On the whole, the plots for eigenfrequencies $\Omega_{P1}(x^1)$ and $\Omega_{T1}(x^1)$ describe well enough their behaviour in the dayside magnetosphere, including the abrupt changes at the plasmapause ($L \approx 4$). When approaching the magnetopause ($L \approx 10$), the applicability of the chosen magnetospheric model is inevitably called into question. Therefore, the behaviour of all the computed functions should be regarded only as probable, when approaching the magnetopause.

Our previous paper (Leonovich and Mazur, 1993) has shown that, for an axisymmetrical model of the magnetosphere with cold plasma at rest, the inequality $\Delta\Omega_N=\Omega_{TN}-\Omega_{PN}>0$ holds everywhere. Figure 3 shows that in the case of a moving-plasma model balanced by the plasma pressure gradient, this inequality is reversed in the outer magnetosphere ($L>8$). The behaviour of Ω_{PN} is essentially determined by the the azimuthal wave number m. In a cold quiescent plasma, as well as in a plasma with finite pressure, poloidal eigen oscillations may be excited on each magnetic shell by the single frequency $\bar{\omega}=\Omega_{PN}$, independent of their azimuthal structure. In a moving plasma the azimuthal harmonic with a certain m has its own distinctive frequency $\Omega_{PN} \equiv \Omega_{PNm}$ on each magnetic shell. This distinction is stronger, the greater the plasma rotation velocity gradient $\nabla_1\Omega$. The highest gradient $\nabla_1\Omega$ is reached in the transition region between the magnetosphere and the solar wind.

One can see that azimuthal harmonics with $m<0$ in the transition region have a local maximum in the distribution of eigenfrequencies. This may result in poloidal Alfvén eigen oscillations confined between two poloidal turning points (Leonovich and Mazur, 1995). In other words, the local maximum $\Omega_{PNm}(x^1)$ acts as a resonator for such oscillations. Another interesting feature involves azimuthal harmonics with $m>0$. It is evident from Fig. 3 that corresponding eigenvalues Ω_{PNm} are cut off on some shell $L=L_{mc}$, even before reaching the magnetopause. This is related to the free-term coefficient in Eq. (11) having a local minimum on parameter $\bar{\omega}$ below which the frequency eigenvalue Ω_{PNm} cannot drop. For real values of $\bar{\omega}$ no solutions exist for Eq. (11) on magnetic shells larger than L_{mc}, satisfying the given boundary conditions. Again, we wish to emphasise that it is in this region that the applicability of the model magnetosphere that we employ is rather problematic.

The $\Delta_1(x^1)$ curve in Fig. 3 is displayed as a piecewise smooth function. This is related to the fact that the definition $\Delta_N(x^1)$ itself suggests a possibility of the horizontal
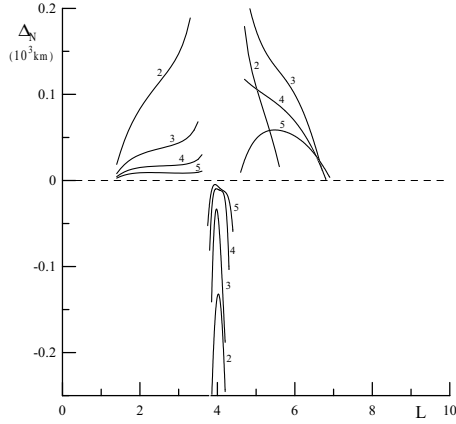
Fig. 5. Dependency of resonant magnetic surface splitting Δ_N (equatorial distance between poloidal and toroidal resonant surfaces) on magnetic shell parameter L for the longitudinal harmonics $N=2, 3, 4, 5$. In the range of magnetic shells studied, Δ_N practically does not depend on the azimuthal wave number m.

line $\bar{\omega}=$const intersecting the curves of the two functions $\Omega_{PN}(x^1)$ and $\Omega_{TN}(x^1)$. As can be seen from the figure, it is not always possible. Moreover, when deriving the expression for $\Delta_N(x^1)$, we used the linear expansions $\Omega_{PN}(x^1)$ and $\Omega_{TN}(x^1)$, inapplicable near the extrema of these functions. At point $L=L_0$, where the curves intersect, $\Delta_N=0$. When $L>L_0$, the concept of resonant shell splitting becomes inapplicable. Since the curves $\Omega_{PNm}(x^1)$ and $\Omega_{TN}(x^1)$ diverge greatly, the horizontal line intersecting $\Omega_{PNm}(x^1)$ will not intersect $\Omega_{TN}(x^1)$ anywhere before the magnetopause. Values of Δ_1 shown in Fig. 3 correspond to the equatorial splitting of resonant surfaces. When projected onto the ionosphere along field lines the value of Δ_1 drops 10- (on $L=3$) to 40-fold (on $L=8$).

Figure 4 displays the curves for eigenfrequencies $f_{(T,P)N}=(\Omega_{(T,P)N}+m\Omega)/2\pi$ for the first five harmonics of toroidal and poloidal standing Alfvén waves with azimuthal wave numbers $m=\pm50$. These curves provide some insight into how high the frequency of oscillations should be in the source coordinate system (in the ionosphere), in order to excite poloidal oscillations with $\Omega_{PN}=\bar{\omega}$ in the magnetosphere, which later transform into toroidal oscillations with $\Omega_{TN}=\bar{\omega}$. One can see how greatly the curves $f_{(T,P)N}(x^1)$ diverge on shells corresponding to the outer magnetosphere, for different signs of the azimuthal wave number m. To generate waves travelling in the magnetosphere azimuthally, in the direction of plasma rotation ($m>0$), the source frequency ω must be higher than the frequency of the opposite-propagating waves ($m<0$). One implication is that oscillations standing on the azimuthal coordinate cannot settle in a magnetosphere with moving plasma.

Figure 5 shows the dependencies of the equatorial distance between the poloidal and toroidal resonant surfaces Δ_N on L for the standing Alfvén waves' harmonics $N=2, 3, 4, 5$. They, as well as Δ_1, are represented by piecewise smooth functions in the regions of the magnetosphere where one can
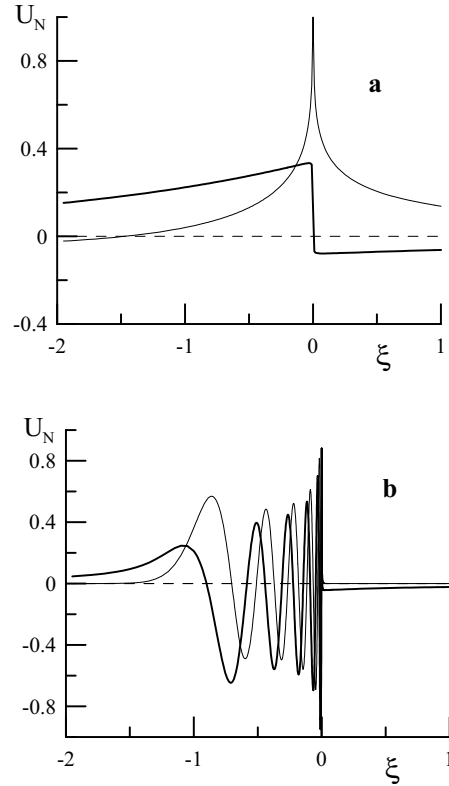

Fig. 6. The structure of standing Alfvén waves across magnetic shells in two limiting cases. The upper plot (**a**) shows dependencies of the U_N function's real (thick line) and imaginary (thin line) components describing the structure of "field line resonance"-type oscillations with $\kappa_N=0.1$. The lower plot (**b**) shows the U_N function's real and imaginary components describing the structure of "travelling wave"-type oscillations with $\kappa_N=20$.

speak of resonant surface splitting. One of the peculiarities of these curves which should be taken notice of is the very small value of the parameter $L_0\approx6$, on whose magnetic shell the curves Ω_{P2} and Ω_{T2} intersect. For the other harmonics $L_0\approx7-8$. Comparing Fig. 5 with Fig. 3, one can observe that the characteristic values of Δ_N listed in Fig. 5 are 1–2 orders lower than Δ_1. This is what constitutes the uniqueness of the basic harmonic. It appears to be the only harmonic for which, with realistic values of m and γ_N in the magnetosphere, the "travelling wave"-type structure can be expected across magnetic shells.

The corresponding values of the critical azimuthal wave number m_{cN}, for which a transition takes place from the "travelling wave"-type structure to the "field line resonance"-type structure of standing waves, are given in Fig. 7. The m_{c1} for the basic harmonic is so different from all the other m_{cN} ($N=2, 3...$) values, that comparing them in one plot requires a logarithmic scale. Note that for oscillations with a conspicuous enough "travelling wave" structure, the condition $m\gg m_{cN}$ must be met. Characteristic values of m in MHD oscillations observed in the magnetosphere rarely exceed $m=200$. Figure 7 implies that the condition $m\gg m_{cN}$ can
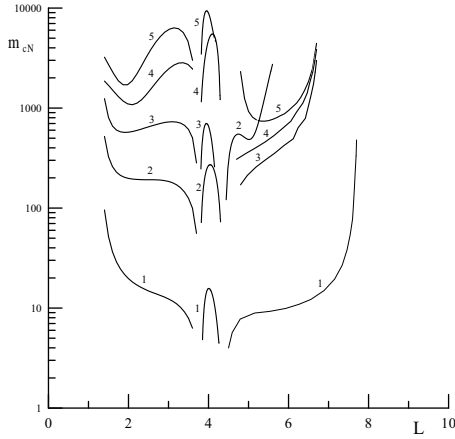
Fig. 7. Dependency of the critical value of the azimuthal wave number m_{cN} for the first five parallel harmonics of standing Alfvén waves. The $m>m_{cN}$ values correspond to $\kappa_N>1$, when the structure of oscillations across magnetic shells has the form of a "travelling wave". The $m<m_{cN}$ values correspond to $\kappa_N<1$, when the structure of oscillations has the "field line resonance" form.
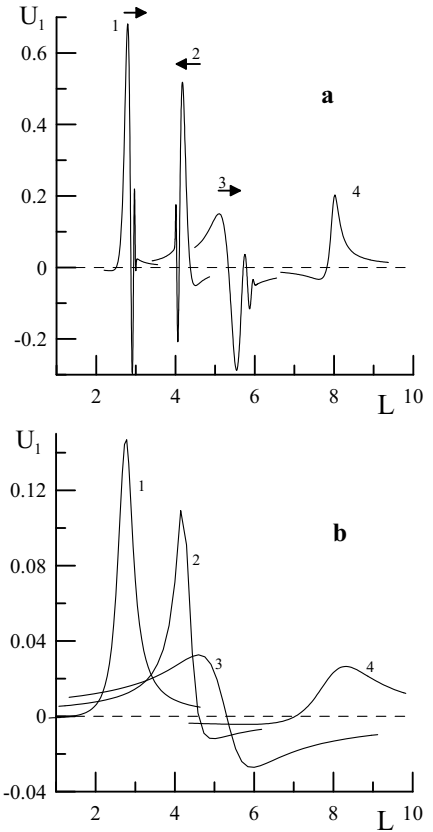

Fig. 8.   The transverse structure of the first longitudinal harmonic of standing Alfvén waves ($N=1$) with azimuthal wave number $m=100$, excited on 4 different magnetic shells ($L=3$, 4, 6, 8) by ionospheric external currents of equal density. **(a)** shows oscillations with moderate damping ($\epsilon=0.1$), while **(b)**, those with small damping ($\epsilon=10^{-2}$). Arrows in Fig. 8b indicate the direction in which the wave propagates across magnetic shells.

be satisfied only for the basic harmonic of standing Alfvén waves $N=1$.

Figure 8 presents the transverse structure of the basic harmonic with azimuthal wave number $m=100$. Various patterns are covered regarding oscillations generated in various regions of the magnetosphere by ionospheric currents of equal intensities. The density $j_\parallel$ of external parallel currents is chosen such that, for shell $L=3$, the parameter b_1 determining the oscillation amplitude (see Eq. 26) should be equal to unity. Meanwhile, the characteristic ratios of the oscillation amplitudes (e.g. magnetic field amplitudes) in Fig. 8 are as they would be near the ionosphere.

Figure 8a displays the transverse structure of oscillations with moderate damping ($\gamma_N=10^{-1}\bar{\omega}$). The oscillations have a typically resonance-type structure on all magnetic shells. Their amplitude is small enough. Such oscillations have toroidal polarisation near the amplitudinal resonance maximum. A characteristic localisation scale $\bar{x}^1\sim\gamma_N L/\bar{\omega}$ for oscillations across magnetic shells in this case is determined by dissipation. Figure 8b presents the structure of similar oscillations but with small damping ($\gamma_N=10^{-2}\bar{\omega}$). The travelling wave-type structure is clearly manifest on magnetic shells $L\approx 3$, 4, 6. The oscillations' amplitude in the neighbourhood of the poloidal resonant shell, where they are generated, is much greater than near the toroidal one, where they dissipate. Therefore, their overall polarisation may be regarded as poloidal. The wave propagation direction is indicated in Fig. 8b with arrows - from the poloidal resonant surface to the toroidal. On the magnetic shell $L\approx 8$, where the curves $\Omega_{P1}(x^1)$ and $\Omega_{T1}(x^1)$ intersect, and, correspondingly, $\Delta_1\to 0$, the oscillations have a typically resonance structure. Their polarisation near the maximum amplitude is toroidal.

7   The structure of standing Alfvén waves as compared to discrete auroral arcs

Note that the structure of travelling wave-type oscillations is very similar to that observed in discrete auroral arcs associated with multiple inverted V-type structures in the particle flows precipitating into the ionosphere (Nadubovich, 1992; McFadden et al., 1999; Newell, 2000). The characteristic size of such structures across magnetic shells is a few tens of km, to $\sim$100 km at the ionosphere level. The number of structural elements (auroral arcs) observed simultaneously may reach 3–4, with one of the outer arcs being the widest. It is not unusual for such aurorae to have a periodic structure in the azimuthal direction (longitudinally), as well. Characteristic spatial sizes of elements of the azimuthal structure are in the 5–60-km range. Such periodic structures move bodily in the azimuthal direction with velocities of $\sim$1 km/s: westwards before local midnight, eastwards after midnight. This is approximately consistent with the magnetospheric plasma convection velocity, as projected onto the ionosphere along geomagnetic field lines.

Since aurorae are related to charged particle flows from the magnetosphere into the ionosphere, the latter enjoys enhanced conductivity in the precipitation area. On the one hand, this promotes generation of external ionospheric currents – Alfvén wave sources, while on the other hand, it keeps their dissipation small. Moreover, for high-energy particles, the presence of a parallel component in the electric field of the Alfvén waves in question results in structured fluxes of particles precipitating into the ionosphere.

Assume the structure of such aurorae to be related to the way the maximum amplitudes of the above transverse small-scale Alfvén waves are distributed. Given the fact that the observed aurorae are azimuthally structured, it could be expected that typical values of the azimuthal wave number are in the range $m{\sim}100{-}1000$. The Alfvén oscillations' azimuthal phase velocity is $v_\phi = \omega\rho/m$. As Fig. 3 implies, at latitudes corresponding to the auroral region ($\theta{\sim}65°{-}70°$, $\rho = R_E\cos\theta{\sim}3000\,\text{km}$), the characteristic eigenfrequency of the standing Alfvén waves' basic harmonic is $\omega{\sim}0.05\,\text{rad/s}$ in our model magnetosphere with a dipole magnetic field. Since the azimuthal velocities observed in auroral propagation $v_\phi{\sim}1\,\text{km/s}$, the velocities of the associated oscillations cannot significantly exceed this value. For oscillations propagating along the ionosphere with a speed close to the ionospheric convection velocity, this corresponds to an azimuthal wave number $m{\sim}100$. With the azimuthal wave number increasing, the oscillations' azimuthal phase velocity declines, dropping below the magnetospheric plasma convection velocity.

The same Fig. 3 also implies that the typical equatorial splitting of resonant magnetic shells is $\Delta_1{\sim}2000\,\text{km}$. Mapped along the dipole magnetic field lines, this becomes ${\sim}60{-}70\,\text{km}$ at the ionosphere level. In the magnetosphere's midnight sector, with field lines stretching in the geomagnetic tail, this value can be even smaller, quite consistent with the typical auroral arc widths. Assuming the structure of oscillations to resemble that presented in Fig. 8b, the maximum near the poloidal resonant magnetic shell is the widest. When approaching the toroidal magnetic shell, the width of the amplitude maxima decreases with the changing radial wavelength of the oscillations. Such a (poleward or equatorward) shift on the ionosphere can take any direction, depending on the resonant surfaces' mutual locations in the magnetosphere. Note that the structure of oscillations in Fig. 8b refers to the lower limit of the admissible azimuthal wave number range $m{\sim}100$. Aurorae appearing thanks to Alfvén oscillations with azimuthal wave numbers considerably exceeding this minimum value cannot be ruled out. With m increasing, the width of each separate auroral arc diminishes, while the number of such arcs grows, resulting, apparently, in an inability to visually resolve separate arcs.

One of the implications of this interpretation is a possible periodic variation (with periods of Alfvén oscillations ${\sim}100\,\text{s}$) in the brightness of aurorae – their actual characteristic feature. Besides, periodic alternations (with the same period of ${\sim}100\,\text{s}$) of dark arcs and auroral arcs should be observed, consistent with a periodically changing sign of

$E_\parallel$ in the even and odd periods of the latitudinal distribution of the standing Alfvén waves' amplitudes. Admittedly, the above presented pattern concerns the structure of only one harmonic of standing Alfvén waves generated by a monochromatic source with the azimuthal wave number m. Many of such harmonics can be excited in the magnetosphere with different wave numbers m and corresponding eigenfrequencies. Therefore, the pattern of the associated aurorae can be much more diverse.

8   Conclusions

Listed below are the major results of this work.

1. Equation (8) was derived describing the structure of standing Alfvén waves with high azimuthal wave numbers $m{\gg}1$ in a dipole magnetosphere with rotating plasma.

2. Solutions were found to Eqs. (11) and (16), defining the longitudinal (along magnetic field lines) structure and spectrum of the eigenfrequencies of poloidal and toroidal Alfvén oscillations in the magnetosphere. Equations (15) and (20) have been obtained, describing the transverse (across magnetic shells) structure of standing Alfvén waves in the magnetosphere with rotating plasma near the poloidal and toroidal resonant surfaces.

3. A model Eq. (21) was constructed, allowing for defining the transverse structure of Alfvén oscillations under study, not only near resonant surfaces, but in the entire region of existence, as well. An analytical solution (26) was produced for this equation. A comparative analysis was performed for the transverse structure of oscillations excited in various regions of the magnetosphere by ionospheric external currents of equal intensities.

4. The structure of observed discrete auroral arcs was compared to the structure of standing Alfvén waves with high azimuthal wave numbers $m{\sim}100{-}200$. The characteristic transverse size of the localisation region of such oscillations as mapped onto the ionosphere, ${\sim}100\,\text{km}$, was shown to coincide with the characteristic width of the region occupied by discrete auroral arcs. The longitudinal periodicity in aurorae which is sometimes observed can be interpreted as betraying the azimuthal structure of standing Alfvén waves with wave numbers $m{\sim}10^2{-}10^3$. The characteristic azimuthal propagation velocities of aurorae tally with the azimuthal phase velocities of Alfvén waves with $m>100$. The number of observed auroral arcs $\leq 3{-}4$ is roughly the same as the number of amplitude maxima of the basic harmonic of standing Alfvén waves with $m{\sim}100$, across magnetic shells. The presence of a parallel electric field component in these oscillations, for high-energy particles leads, to a periodically increased

flow of charged particles precipitating into the ionosphere and to the attendant brightness variations in the aurorae.

References

Allan, W. and Manuel, J. R.: Ponderomotive effects in magnetospheric waves, Ann. Geophys., 14, 893–905, 1996.

Allan, W., White, S. P., and Poulter, E. M.: Impulse-excited hydromagnetic cavity and field line resonance in the magnetosphere, Planet. Space Sci., 34, 371–380, 1986.

Bespalov, P. A. and Chugunov, Yu. V.: The model of atmospheric electricity from a planetary generator and low-latitude thunderstorm currents (in Russian), Izv. Vuzov, Radiofizika, 40, 99-111, 1984.

Chen, L. and Cowley, S. C.: On field line resonances of hydromagnetic Alfvén waves in a dipole magnetic field, Geophys. Res. Lett., 16, 895–897, 1989.

Chen, L. and Hasegawa, A.: A theory of long period magnetic pulsation. 1. Steady state excitation of field line resonances, J. Geophys. Res., 79, 1024-1032, 1974.

Dungey, J. W.: Electrodynamics of the outer atmospheres, Ionos. Sci. Rep., 69, Ionos. Res. Lab., Cambridge, Pa., 1954.

Frycz, P. , Rankin, R., Samson, J. C., and Tikhonchuk, V. T.: Nonlinear field line resonances: dispersive effects, Phys. Plasmas, 5, 3565-3574, 1998.

Goertz, C. K.: Kinetic Alfvén waves on auroral field lines, Planet. Space Sci., 32, 1387-1392, 1984.

Hasegawa, A.: Particle acceleration by MHD surface wave and formation of aurorae, J. Geophys. Res., 81, 5083-5090, 1976.

Klimushkin, D. Yu.: Spatial structure of transversally small-scale hydromagnetic waves in a plane finite-beta model magnetosphere, Planet. Space Sci., 45, 269-279, 1997.

Korn, G. A. and Korn, T. M.: Mathematical handbook for scientists and engineers, McGraw-Hill Book Company, 1968.

Krylov, A. L., Lifshitz, A. E., and Fedorov, E. N.: On resonance properties of the magnetosphere (in Russian), Izv. Akad. Nauk SSSR, Ser. Fiz. Zemli, 6, 49-58, 1981.

Leonovich, A. S. and Mazur, V. A.: Resonance excitation of standing Alfvén waves in an axisymmetric magnetosphere (monochromatic oscillations), Planet. Space Sci., 37, 1095-1108, 1989.

Leonovich, A. S. and Mazur, V. A.: A theory of transverse small-scale standing Alfvén waves in an axially symmetric magnetosphere, Planet. Space Sci., 41, 697-717, 1993.

Leonovich, A. S. and Mazur, V. A.: Magnetospheric resonator for transverse-small-scale standing Alfvén waves, Planet. Space Sci., 43, 881-883, 1995.

Leonovich, A. S. and Mazur, V. A.: Penetration to the Earth's surface of standing Alfvén waves excited by external currents in the ionosphere, Ann. Geophys., 14, 545–556, 1996, **SRef-ID: 1432-0576/ag/1996-14-545**.

Leonovich, A. S. and Mazur, V. A.: A model equation for monochromatic standing Alfvén waves in the axially symmetric magnetosphere, J. Geophys. Res., 102, 11 443-11 456, 1997.

Leonovich, A. S. and Mazur, V. A.: Structure of magnetosonic eigenoscillations of an axisymmetric magnetosphere, J. Geophys. Res., 105, 27 707-27 716, 2000.

Leonovich, A. S., Mazur, V. A., and Cao, J. B.: Self-consistent model of a dipole-like mrgnetosphere with an azimuthal solar wind flow, J. Plasma Physics., 70, 99-111, 2004.

McFadden, J. P., Chaston, C., and Ergun, R. E.: Microstructure of auroral acceleration region as observed by FAST, J. Geophys. Res., 104, 14,453-14,480, 1999.

Nadubovich, Yu. A.: Morphological investigations of aurorae (in Russian), Nauka, Novosibirsk, 1992.

Newell, P. T.: Reconsidering the inverted-V particle signature: relative frequency of large-scale electron acceleration events, J. Geophys. Res., 105, 15 779-15 794, 2000.

Pilipenko, V. A.: ULF waves on the ground and in space, J. Atmosph. Terr. Phys., 52, 1193-1209, 1990.

Radoski, H. R.: Highly asymmetric MHD resonances, The guided poloidal mode, J. Geophys. Res., 72, 4026-4033, 1967.

Radoski, H. R. and Carovillano, R. R.: Axisymmetric plasmasphere resonance, Toroidal mode, Phys. Fluids, 7, 285-297, 1969.

Rankin, R., Frycz, P., Tikhonchuk, V. T., and Samson, J. C.: Near standing shear Alfvén waves in the Earth's magnetosphere, J. Geophys. Res., 99, 21 291-21 301, 1994.

Rankin, R., Samson, J. C., and Tikhonchuk, V. T.: Parallel electric fields in dispersive shear Alfvén waves in the dipolar magnetosphere, Geophys. Res. Lett., 26, 3601-3604, 1999.

Rankin, R., Lu, J. Y., Marchand, R., and Donovan, E. F.: Spatiotemporal characteristics of ultra-low frequency dispersive scale shear Alfvén waves in the Earth's magnetosphere, Phys. Plasmas, 11, 1268-1276, 2004.

Samson, J. C., Rankin, R., and Tikhonchuk, V. T.: Optical signatures of auroral arcs produced by field line resonances: comparison with satellite observations and modeling, Ann. Geophys., 21, 933–945, 2003, **SRef-ID: 1432-0576/ag/2003-21-933**.

Soldatkin, A. O. and Chugunov, Yu. V.: Unipolar induction as origin of generation of electric fields and currents in plasmaspheres of planets, J. Atmos. Solar-Terr. Phys., 45, 821-831, 2003.

Southwood, D. J.: Some features of field line resonances in the magnetosphere, Plahet. Space Sci., 22, 483-492, 1974.

Southwood, D. J. and Kivelson, M. G.: The effect of parallel inhomogeneity of magnetospheric hydromagnetic wave coupling, J. Geophys. Res., 91, 6871-6877, 1986.

Tikhonchuk, V. T. and Rankin, R.: Electron kinetic effects in standing shear Alfvén waves in the dipolar magnetosphere, Phys. Plasmas, 7, 2630-2645, 2000.

Watt, C. E. J., Rankin, R., and Marchand, R.: Kinetic simulations of electron response to shear Alfvén waves in magnetospheric plasmas, Phys. Plasmas, 11, 1277-1284, 2004.

Wright, A. N.: Coupling of fast and Alfvén modes in realistic magnetospheric geometries, J. Geophys. Res., 97, 6429-6438, 1992.